An in situ set up for the detection of CO(2) from catalytic CO oxidation by using planar laser-induced fluorescence.

Zetterberg, Johan; Blomberg, Sara; Gustafson, Johan; Sun, Zhiwei; Li, Zhongshan; Lundgren, Edvin; Aldén, Marcus

Published in:
Review of Scientific Instruments

DOI:
10.1063/1.4711130

2012

AIP | Review of Scientific Instruments

An in situ set up for the detection of CO2 from catalytic CO oxidation by using planar laser-induced fluorescence

J. Zetterberg, S. Blomberg, J. Gustafson, Z. W. Sun, Z. S. Li et al.

Citation: Rev. Sci. Instrum. **83**, 053104 (2012); doi: 10.1063/1.4711130
View online: http://dx.doi.org/10.1063/1.4711130
View Table of Contents: http://rsi.aip.org/resource/1/RSINAK/v83/i5
Published by the American Institute of Physics.

An *in situ* set up for the detection of CO_2 from catalytic CO oxidation by using planar laser-induced fluorescence

J. Zetterberg,[1,a)] S. Blomberg,[2] J. Gustafson,[2] Z. W. Sun,[1] Z. S. Li,[1] E. Lundgren,[2] and M. Aldén[1]
[1]*Division of Combustion Physics, Lund University, Lund 221 00, Sweden*
[2]*Division of Synchrotron Radiation Research, Lund University, Lund 221 00, Sweden*

(Received 29 February 2012; accepted 15 April 2012; published online 4 May 2012)

We report the first experiment carried out on an *in situ* setup, which allows for detection of CO_2 from catalytic CO oxidation close to a model catalyst under realistic reaction conditions by the means of planar laser-induced fluorescence (PLIF) in the mid-infrared spectral range. The onset of the catalytic reaction as a function of temperature was followed by PLIF in a steady state flow reactor. After taking into account the self-absorption of CO_2, a good agreement between the detected CO_2 fluorescence signal and the CO_2 mass spectrometry signal was shown. The observed difference to previously measured onset temperatures for the catalytic ignition is discussed and the potential impact of IR-PLIF as a detection technique in catalysis is outlined. © *2012 American Institute of Physics*. [http://dx.doi.org/10.1063/1.4711130]

I. INTRODUCTION

Laser diagnostic techniques have been developed during the last decades and have aided in the understanding of combustion phenomena, especially for gas phase analysis. The major benefits with laser diagnostics are the prospect of high spatial and temporal resolution as well as the possibility to measure *in situ*, non-intrusively. Quantities measurable with laser diagnostics are species concentrations, velocities, and particle characteristics.[1–4] Among the available laser diagnostic techniques, laser-induced fluorescence (LIF) has attracted most attention. This is mainly due to its versatility and its high signal strength, making two-dimensional measurements possible. Thus LIF has been used successfully in several areas including atmospheric sciences and medicine.[5,6]

Catalytic reactions play a crucial role in exhaust gas treatment to reduce the emission of harmful gases such as CO, NO, and hydrocarbons (HC) from engines in vehicles. Because of the complex nature of a technical catalyst, most catalysts in use have almost exclusively been developed by trial and error approaches. Their catalytic properties such as activity and selectivity have been probed by mass spectrometry (MS) detecting the gas composition after that the gas has traveled through the catalyst.

With the exception of NO, most gases relevant to exhaust gas treatment, pose no or no easily accessible transitions in the UV-visible spectral range. Two-photon excitation of CO in the UV is plausible, as demonstrated in flames[7–13] and even shown in an SI-engine,[14] but by probing ro-vibrational transitions in the infrared (IR), CO and the other species referred to can be detected. Earlier, this has only been possible for line of sight absorption measurements.

In earlier studies related to catalysis, LIF has been used to study the formation of gas phase OH as an intermediate in flameless oxidation of H_2 by O_2 close to a Pt catalyst.[15–20] Furthermore, two-dimensional LIF of gas phase species above catalytic samples has been used to study the OH formation from O_2 and H_2O, as well as the formation of formaldehyde above Pt catalysts.[21,22] However, due to limitations of detectors, light sources in the mid-infrared spectral range, and to difficulties with thermal background radiation, point measurements as well as two-dimensional visualization of CO_2, CO, and smaller HC have eluded the scientific community for decades.

With the development of new light sources and detectors the area opened up in the late 1990s. Kirby *et al.* published the first two-dimensional measurements of CO in 1999 (Ref. 23) using planar laser-induced fluorescence (PLIF), and introduced applications for non-reacting flows. This effort was followed up by the same group and complemented with CO_2.[24–26] The number of detected species was then extended to smaller hydrocarbons by Li *et al.*[27] For point measurements, polarization spectroscopy of CO_2 was demonstrated by Roy *et al.*[28] and followed up by Alwahabi *et al.*[29] who also compared LIF and polarization spectroscopy in a later work.[30] Taking advantage of the coherent nature of polarization spectroscopy, measurements of nascent CO_2 and H_2O in a flame was published by Li *et al.*[31], but two-dimensional measurements in background-challenging environments were still lacking. The feasibility of CO_2 visualization was tested in a small Briggs-Stratton engine during the exhaust cycle together with a study of the emission from thermally excited CO_2.[32] This gave promise of CO_2 measurements at elevated background temperatures. To the knowledge of the authors, no studies of the CO_2 production by a CO oxidation catalyst have so far been performed by use of PLIF.

In this work we present 2D visualization of the CO_2 distribution during the oxidation of CO by O_2 close to catalysts at elevated temperatures (20-550 °C). By excitation at ~2.7 μm and detection at 4.3 μm, we demonstrate high spatial and temporal resolution of the CO_2 detection. By

a)Author to whom correspondence should be addressed. Electronic mail: johan.zetterberg@forbrf.lth.se.

time-gating, spectral filtering, and thermal background subtraction, single shot images of CO_2 were obtained with good signal quality.

We demonstrate the feasibility of measuring CO_2 concentration close to a single crystal model-catalyst Rh(553) during the CO oxidation by comparing the fluorescence signal, after taking into account the self-absorption of CO_2, to MS-data.

The presented PLIF data together with other techniques such as x-ray photoelectron spectroscopy (XPS), x-ray diffraction (XRD), and scanning tunneling microscopy (STM) provides a more complete picture of the catalytic process, and in particular the almost unknown gas distribution within the used reactor cells.[33]

II. EXPERIMENTAL SETUP

The main part of the reactor cell is a CF40 cube with two CaF_2 viewports opposite to each other, for letting the laser beam in and out, and one perpendicular for the fluorescence signal, as shown in Fig. 1. The top flange has homemade feedthroughs for heating wire electrodes and thermocouple. In order to avoid problems with oxidation, the power feedthroughs are made of Ta, and to avoid problems with Ni carbonyls, the thermocouple is of type C. Commercial type C thermocouple feedthroughs are made of a compensating material that includes Ni. We have therefore made special feedthroughs with real type C thermocouple wire. The thermocouple wire is spot welded to the sample, which is heated by a boralectric heater (Métaux Céramiques Systèmes Engineering). The gas inlet and outlet are placed in the bottom of the chamber together with a pressure gauge and a leak valve controlling the amount of gas let into the mass spectrometer (Pfeiffer PrismaPlus QMG220) for monitoring the overall species concentration. The mass spectrometer was operated at a pressure of 5×10^{-6} mbar and calibrated against a known gas mixture in the reactor cell. The total reactor volume is about 200 ml.

The gas flow is controlled individually by separate mass flow controllers (Bronkhorst EL-FLOW, 50 mln/min). The mixing of the gases is ensured by flowing them through a 4 m-long pipe before entering the reactor cell. The gas pressure in the reactor is controlled by a digital pressure controller (Bronkhorst EL-PRESS).

In the experiments a single-longitudinal-mode Nd:YAG laser (Spectra Physics, PRO 290-10), operating at a repetition rate of 10 Hz and with an 8 ns pulse length, was utilized. The second harmonic at 532 nm was used to pump a tunable dye laser (Sirah PRSC-D-18) operating with LDS 765 as dye. The residual of the fundamental beam (at 1064 nm) after the frequency doubling was difference frequency mixed with the output of the dye laser (at ~763 nm) in a $LiNbO_3$ crystal, yielding a tunable infrared laser beam at ~2.7 μm, with a pulse energy of 5-8 mJ and a 5 ns pulse length. The bandwidth of the infrared laser beam was estimated in an earlier work to be 0.025 cm^{-1}.[31] The experimental setup is shown in Fig. 1.

The infrared laser beam was formed into a laser sheet (~6 mm high) by a cylindrical and a spherical lens, $f = -40$ mm and $f = 150$ mm, respectively, and were sent through the cell directly underneath the catalyst. The fluorescence signal was collected by a CaF_2 lens at 90° to the incident laser sheet through a narrowband, liquid nitrogen cooled, interference filter (centered at 4.26 μm) and detected by a 256 × 256 InSb IR camera (Santa Barbara Focal Plane, SBF LP134). In order to discriminate the thermal background the camera was triggered at 20 Hz, via a digital delay generator (Stanford Research systems DG535), every second exposure synchronized with the laser (laser runs 10 Hz). In this way the thermal background could be subtracted. The long radiative lifetime (~100 μs) of the IR-transitions[25,34,35] were utilized to discriminate laser background and time jitter, by using a 15 μs time delay relative to the Q-switch of the laser. The trigger scheme can be seen in Fig. 2, the laser sets the start time, the fluorescence appears almost instantly, the camera is then triggered 15 μs after the opening of the laser Q-switch. The exposure time for the camera is optimized to discriminate background and favor fluorescence signal and set to 15 μs. The camera is then triggered once more during the cycle 50 ms after the first exposure, camera gate unchanged. This is to collect the thermal background without any influence of the laser, 100 ms after the first lasershot the next cycle starts, again with the opening of the laser Q-switch.

The excitation wavelength was determined by making an excitation scan of the $(00^00) \rightarrow (10^001)$ transition (3690-3725 cm^{-1}) of an open air CO_2 jet. The lines were assigned and wavelength calibrated using line positions as reported by

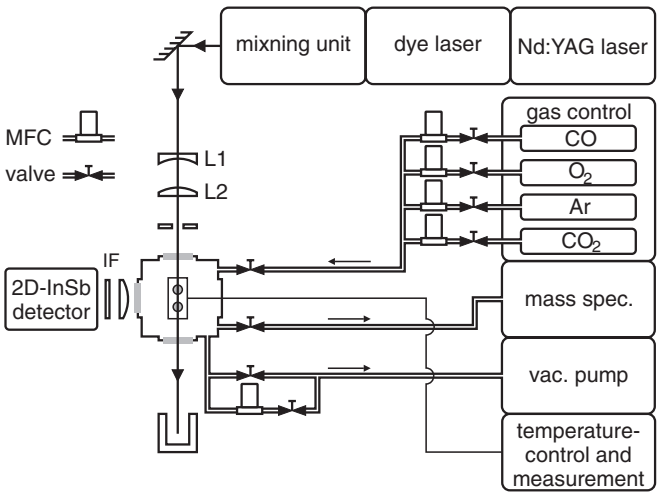

FIG. 1. Schematic of the experimental set up.

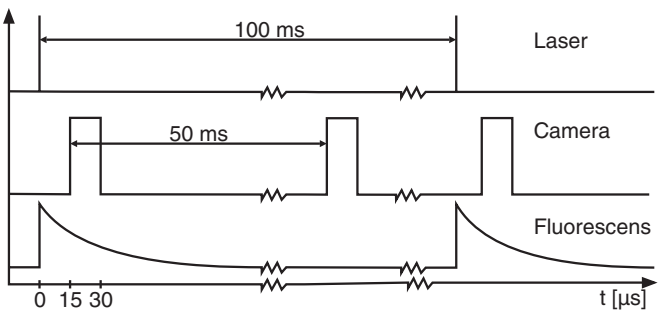

FIG. 2. Schematic of the trigger scheme.

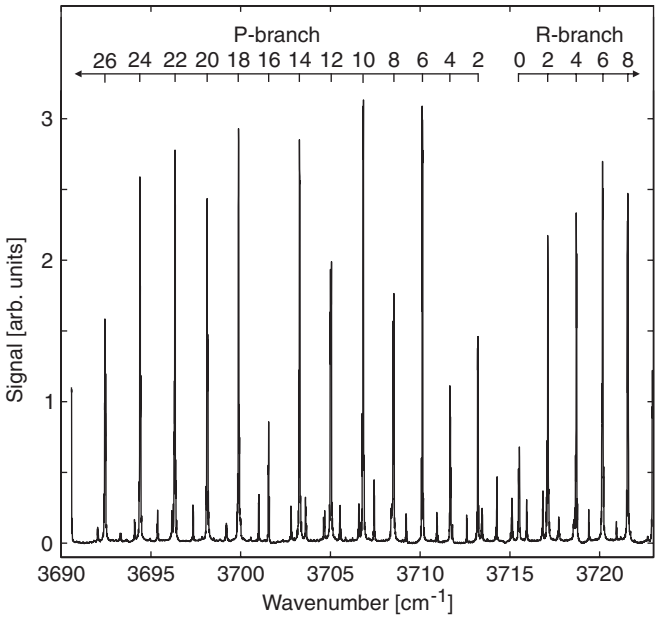

FIG. 3. CO_2 spectrum where the lines for the $(00^00) \rightarrow (10^001)$ transition are assigned. The smaller peaks are overtones and are not relevant to this work. P(12) was used for the fluorescence measurements.

Deeley and Jones.[36] A suitable ro-vibrational line, without interference, was chosen. In the single-crystal Rh(553) measurements described here the P12-line was chosen after simulations based on the HITRAN database[37] at different expected gas temperatures. The spectrum from the excitation scan at room temperature can be seen in Fig. 3.

III. RESULTS AND DISCUSSION

The measurements were performed below a Rh(553) surface and were conducted in a flow reactor mode although the flow was kept very low, with the purpose not to exchange the gas but to ensure a constant pressure (varying from 100 mbar to 200 mbar between different measurement sets) with known concentrations, minimizing the effect of a small possible leakage. These measurements were conducted at fixed temperature steps at steady state conditions, making it possible to average the fluorescence signal. The data were collected by the IR-camera, 1000 images per data point with every second image being without fluorescence in order to be able to subtract the thermal background. The thermal background was several hundred times stronger than the fluorescence signal, completely obscuring the fluorescence signal. The thermal background image, however, is acquired so close in time to the data image (~50 ms) that the temperature between the two can be considered stable. The correction for laser sheet inhomogeneity was made by acquiring a fluorescence image at a known CO_2 concentration. This means that stable artifacts in the sheet was corrected for but shot-to-shot fluctuations were not taken into account.

The signal-to-noise ratio for single-shot measurements was briefly investigated and a single shot image is shown in Fig. 4, although the image has considerable noise the CO_2 profile underneath the catalyst is clearly visible. The signal-to-noise is sufficient for CO_2 visualization but not for an estimate of the concentration.

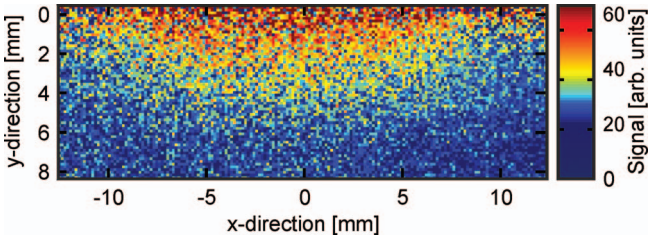

FIG. 4. Single-shot image (15 μs exposure time) of the CO_2 distribution underneath a Rh(553) catalyst at a total pressure of 100 mbar with 60 mbar of CO and 40 mbar of O_2.

To give an estimation of the concentration an absolute calibration of the CO_2 concentration was attempted. This was done on averaged data (500 background subtracted single-shots) in order to minimize the influence of shot-to-shot fluctuations. By calibrating the fluorescence signal for known CO_2 concentrations and using a kernel density estimation based on Eq. (2) below for the self-absorption (both from produced CO_2 in the cell and naturally abundant CO_2 in the air outside the cell) but assuming the quenching related to different collisional partners being constant (the overall pressure was kept constant). The absorption through a length l can be described by Beer-Lamberts law

$$I = I_0 \times e^{-\sigma l N}, \tag{1}$$

where I is the intensity after the length l, I_0 the initial intensity, N the number of absorbers, and σ the absorption cross-section. In this case, however, the signal will pass through two lengths with different CO_2 concentrations, yielding in a total signal S that can be described by

$$\left.\begin{aligned} I_1 &= I_0 \times e^{-\sigma l_1 N_1} \\ I_2 &= I_1 \times e^{-\sigma l_2 N_2} \end{aligned}\right\} \Rightarrow S \propto I_2 = I_0 \times e^{-\sigma (l_1 N_1 + l_2 N_2)}, \tag{2}$$

where I_1 and I_2 is the intensity after the cell (length l_1) and in the open air (length l_2), respectively. I_0 is the initial intensity, N_1 and N_2 the number of absorbers in the cell and in the open air, respectively and σ the absorption cross-section for CO_2 at 4.3 μm.

In Fig. 5 are shown the estimated two-dimensional CO_2 concentration at two different temperatures, (c) at 470 °C and d) at 520 °C together with a profile of the concentration (a) at ~3.5 mm below the surface of the Rh(553) crystal as a function of temperature of the crystal. The measurement was made at 100 mbar and in an atmosphere of 60 mbar of CO and 40 mbar of O_2. By comparing the mass spectrometry signal and the estimated CO_2 concentration from the PLIF signal, a good agreement is achieved. The sudden onset of the CO_2 production, i.e., the catalytic ignition, can be easily observed, both in the concentration plots as well as in the 2D infrared images. It can be seen that the activation temperature of the Rh(553) surface occurs at a narrow temperature span starting at around 400 °C.

Further, the two-dimensional measurement of the CO_2 concentration shows, as expected, a gradual decrease in the

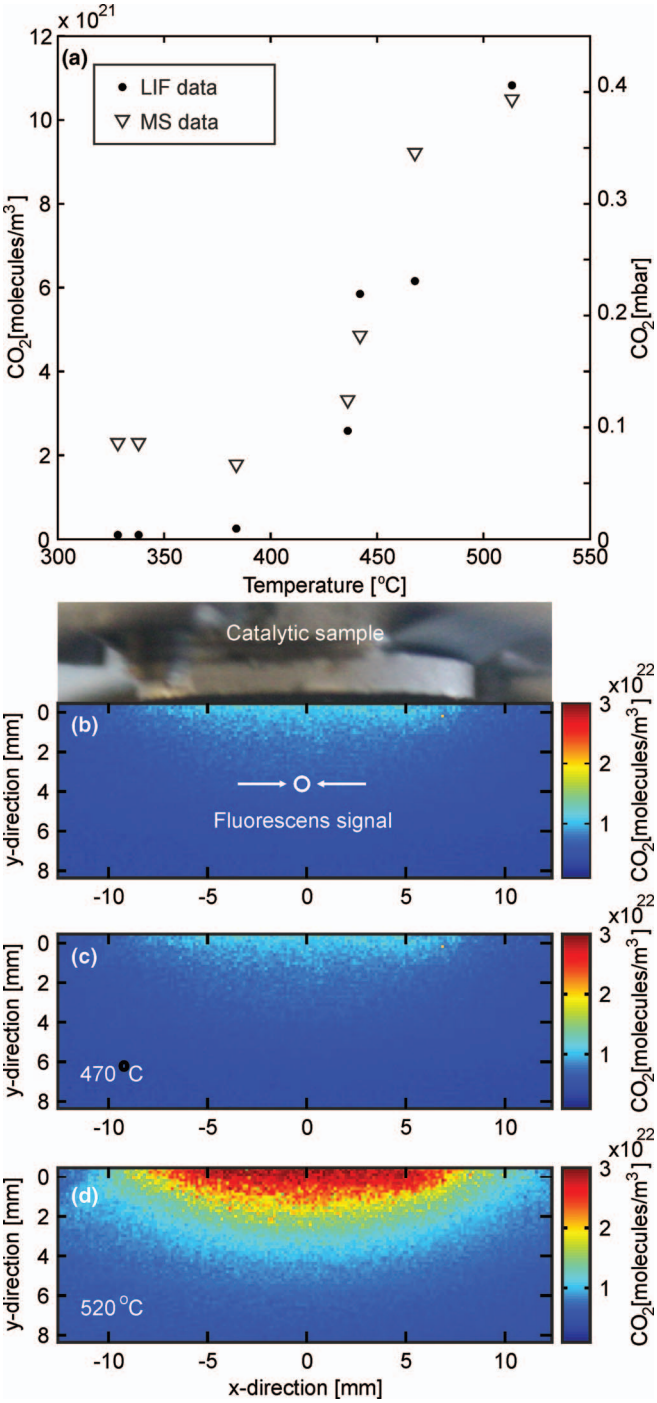

FIG. 5. (a) The CO_2 concentration 3.5 mm below the Rh(553) surface, (b) the position of the catalytic sample and where the fluorescence signal was averaged, (c) an estimate of the CO_2 concentration below the catalyst at 470 °C and (d) an estimate of the CO_2 concentration below the catalyst at 520 °C. The gas composition was 60 mbar of CO and 40 mbar of O_2.

CO_2 concentration as function of the distance from the catalyst surface.

In a previous work by Gustafson *et al.*[38], the activation temperature was observed to be lower, at around 250 °C. Although the present report focuses on the ability to detect CO_2 using PLIF under realistic catalytic conditions, it is interesting to discuss this difference. One reason could be the different reaction conditions used. In the present study, the partial CO pressure was 40 mbar but only 7 mbar in Ref. 38, making CO poisoning of the catalyst surface more effective leading to an increased activation temperature. Another difference is the total pressure (100 mbar in the present study, 500 mbar in Ref. 38), which may also influence the activation temperature. Furthermore, the cleanliness of the surface in the present study is not known, allowing for contaminants to affect the activation temperature. Finally, it should also be noted that a significant amount of uncertainty lies in the temperature measurements, making the absolute activation temperature difficult to determine without introducing large error bars.

IV. SUMMARY

The possibility of visualizing the CO_2 concentration right above a catalyst surface by means of PLIF in the mid-infrared was demonstrated. 2D single-shot measurements were tested and hold promise for future measurements, although the signal-to-noise ratio in the present measurements needs to be improved for accurate single-shot measurements. An estimation of the CO_2 concentration was made and was compared to MS-measurements with good agreement. Future applications might include measuring more than one catalyst simultaneously, at different conditions in order to on-line compare different catalysts making the screening effort to find better catalysts more efficient. The technique can also directly show where the sample is active, e.g., the sample more active on the sides than on the actual surface, something that is impossible to determine with a regular MS-measurements. Finally, the method could also be of significance when studying catalytic reactions in which also gas phase reactions occur, e.g., flameless combustion.

ACKNOWLEDGMENTS

This work was financially supported by the foundation for strategic research (SSF), the Swedish Research Council (VR), the Crafoord Foundation, the Knut and Alice Wallenberg Foundation, the Anna and Edwin Berger Foundation, and the Center of Combustion Science and Technology, CECOST. The authors would also like to thank Jonathan Johnsson for his assistance with the programming of the kernel density estimation.

[1] A. C. Eckbreth, *Laser Diagnostics for Combustion Temperature and Species*. (Abacus, Tunbridge Wells, Kent, Cambridge, Mass., 1988).
[2] K. Kohse-Höinghaus and J. B. Jeffries, *Applied Combustion Diagnostics* (Taylor & Francis, New York, 2002).
[3] J. Wolfrum, Sym. (Int.) Combust., [Proc.] **27**(1), 1–41 (1998).
[4] M. Alden, J. Bood, Z. S. Li, and M. Richter, Proc. Combust. Inst. **33**, 69–97 (2011).
[5] W. Liao, A. T. Case, J. Mastromarino, D. Tan, and J. E. Dibb, Geophys. Res. Lett. **33**(9), L09810, doi:10.1029/2005GL025470 (2006).
[6] S. Svanberg, Phys. Scr. **T19b**, 469–475 (1987).
[7] M. Alden, S. Wallin, and W. Wendt, Appl. Phys. B **33**(4), 205–212 (1984).
[8] N. Georgiev and M. Alden, Appl. Spectrosc. **51**(8), 1229–1237 (1997).
[9] J. Haumann, J. M. Seitzman, and R. K. Hanson, Opt. Lett. **11**(12), 776–778 (1986).
[10] J. M. Seitzman, J. Haumann, and R. K. Hanson, Appl. Opt. **26**(14), 2892–2899 (1987).
[11] D. A. Everest, C. R. Shaddix, and K. C. Smyth, Symposium (International) on Combustion **26**(1), 1161–1162 (1996).

[12]B. B. Dally, A. R. Masri, R. S. Barlow, and G. J. Fiechtner, Combust. Flame **132**(1-2), 272–274 (2003).
[13]J. E. Rehm and P. H. Paul, Proc. Combust. Inst. **28**, 1775–1782 (2000).
[14]M. Richter, Z. S. Li, and M. Alden, Appl. Spectrosc. **61**(1), 1–5 (2007).
[15]E. Fridell, U. Westblom, M. Alden, and A. Rosen, J. Catal. **128**(1), 92–98 (1991).
[16]M. Försth, Ph.D. dissertation, Chalmers University of Technology and Göteborg University, 2001.
[17]M. Försth, F. Gudmundson, J. L. Persson, and A. Rosen, Combust. Flame **119**(1-2), 144–153 (1999).
[18]E. Fridell, A. P. Elg, A. Rosen, and B. Kasemo, J. Chem. Phys. **102**(14), 5827–5835 (1995).
[19]E. Fridell, A. Rosen, and B. Kasemo, Langmuir **10**(3), 699–708 (1994).
[20]F. Gudmundson, J. L. Persson, M. Forsth, F. Behrendt, B. Kasemo, and A. Rosen, J. Catal. **179**(2), 420–430 (1998).
[21]W. Kang, O. Fujita, and K. Ito, ASME J. Energy Resour. Technol.**118**(1), 82–87 (1996).
[22]F. Gudmundson, E. Fridell, A. Rosen, and B. Kasemo, J. Phys. Chem. **97**(49), 12828–12834 (1993).
[23]B. J. Kirby and R. K. Hanson, Appl. Phys. B **69**(5), 505–507 (1999).
[24]B. J. Kirby and R. K. Hanson, Appl. Opt. **40**(33), 6136–6144 (2001).
[25]B. J. Kirby and R. K. Hanson, Proc. Combust. Inst. **28**, 253–259 (2000).
[26]B. J. Kirby and R. K. Hanson, Appl. Opt. **41**(6), 1190–1201 (2002).
[27]Z. S. Li, M. Rupinski, J. Zetterberg, and M. Alden, Proc. Combust. Inst. **30**, 1629–1636 (2005).
[28]S. Roy, R. P. Lucht, and A. Mcilroy, Appl. Phys. B **75**(8), 875–882 (2002).
[29]Z. T. Alwahabi, Z. S. Li, J. Zetterberg, and M. Alden, Opt. Commun. **233**(4-6), 373–381 (2004).
[30]Z. T. Alwahabi, J. Zetterberg, Z. S. Li, and M. Alden, Eur. Phys. J. D **42**(1), 41–47 (2007).
[31]Z. S. Li, M. Rupinski, J. Zetterberg, Z. T. Alwahabi, and M. Alden, Chem. Phys. Lett. **407**(4-6), 243–248 (2005).
[32]Z. S. Li, J. Zetterberg, P. Malm, and M. Aldén, in *European Combustion Meeting* (Louvain-la-Neuve, Belgium, 2005), pp. 6.
[33]S. Matera and K. Reuter, Catal. Lett. **133**(1-2), 156–159 (2009).
[34]J. T. Houghton, P. Phys. Soc. London **91**(572P), 439 (1967).
[35]W. A. Rosser, A. D. Wood, and E. T. Gerry, J. Chem. Phys. **50**(11), 4996 (1969).
[36]C. M. Deeley and J. W. C. Johns, J. Mol. Spectrosc. **129**(1), 151–159 (1988).
[37]L. S. Rothman, I. E. Gordon, A. Barbe, D. C. Benner, P. E. Bernath, M. Birk, V. Boudon, L. R. Brown, A. Campargue, J. P. Champion, K. Chance, L. H. Coudert, V. Dana, V. M. Devi, S. Fally, J. M. Flaud, R. R. Gamache, A. Goldman, D. Jacquemart, I. Kleiner, N. Lacome, W. J. Lafferty, J. Y. Mandin, S. T. Massie, S. N. Mikhailenko, C. E. Miller, N. Moazzen-Ahmadi, O. V. Naumenko, A. V. Nikitin, J. Orphal, V. I. Perevalov, A. Perrin, A. Predoi-Cross, C. P. Rinsland, M. Rotger, M. Simeckova, M. A. H. Smith, K. Sung, S. A. Tashkun, J. Tennyson, R. A. Toth, A. C. Vandaele, and J. Vander Auwera, J. Quant. Spectrosc. Radiat. Transf. **110**(9-10), 533–572 (2009).
[38]J. Gustafson, R. Westerstrom, O. Balmes, A. Resta, R. van Rijn, X. Torrelles, C. T. Herbschleb, J. W. M. Frenken, and E. Lundgren, J. Phys. Chem. C **114**(10), 4580–4583 (2010).